Review

The interaction of formic acid with transition metal surfaces, studied in ultrahigh vacuum

M R Columbia * and P.A Thiel

Department of Chemistry and Ames Laboratory, Iowa State University, Ames, IA 50011 (USA)

(Received 24 February 1993, in revised form 18 August 1993)

Abstract

In this report, we review the interaction of formic acid (HCOOH) with transition metal surfaces, as studied with the tools of modern surface science in an ultrahigh vacuum environment Our goal is to provide a broad overview of the fundamental adsorption and decomposition processes which HCOOH undergoes at the surfaces of these metals The metal substrates include Cu, Fe, W, Ni, Ru, Ag, Pt, Au, Rh and Pd

1. Introduction

The desirability of fuel cells for the direct oxidation of C-containing liquid fuels has provided an impetus for many electrochemical studies of the oxidation of formic acid (HCOOH) Pt electrodes have been the focus of much of this research as far back as the 1920s [1–3] and remain so to the present day, although closely related metals, such as Rh and Pd, have also been subject to significant scrutiny The oxidation of HCOOH at Pt electrodes proceeds with nearly 100% coulombic efficiency, however, the reaction is observed to be self-poisoning [4] Classical electrochemical methods have led most researchers to posit that oxidation involves a "reactive" intermediate that can produce CO_2 and H^+, which desorb, or a "poisoning" intermediate, which remains adsorbed to the electrode surface under operating conditions A prime candidate for the reactive intermediate is carboxylate (COOH), prime candidates for the poison have historically included formyl (CHO), carbon monoxide (CO) and hydroxymethylidyne (COH) [5–8] Recently, *in situ* IR spectrometric techniques have been used to identify the poison as CO [9], although this conclusion is still controversial [10]

The reaction of HCOOH with transition metals also has been an active area of interest within the surface science community since the early 1970s One genesis of this interest lies in the desire to understand fundamental aspects of heterogeneous catalysis, for which HCOOH decomposition serves as a simple model [11,12] Investigations driven by such a motive have typically been performed in reactors which operate at higher pressures (10^{-5}–10^{0} Torr) than those utilized in modern surface science experiments (10^{-10}–10^{-11} Torr) [13] The general consensus from such work is that decomposition on metals can occur via two different pathways [11] The first is dehydrogenation (deprotonation), which produces CO_2 and H_2, the second is dehydration, which produces CO and H_2O (Note that the first reaction, i e dehydrogenation, yields the same species as arise from non-poisoning electrochemical oxidation, whereas dehydration yields a supposed poison, i e CO Thus, it is highly relevant to understand conditions which might favor one reaction over the other) The advent of ultrahigh vacuum (UHV) and its concomitant surface-sensitive analysis techniques has allowed exploration of the mechanisms and intermediates of these paths at the molecular level under well-defined conditions

The techniques which are brought to bear on the problem generally fall into two groups One group consists of thermal desorption spectroscopy (TDS)—also known as temperature-programmed desorption (TPD) and its more complex variant, temperature-pro-

* Present address Department of Chemistry, Indiana–Purdue University, Fort Wayne, Fort Wayne, IN 46805-1499, USA

0022-0728/94/$7 00
SSDI 0022-0728(93)03153-G

grammed reaction spectroscopy (TPRS) This group of techniques serves to identify the gas-phase products of surface adsorption as a function of the surface temperature This identification serves mainly to determine whether decomposition occurs at all and, if so, whether it proceeds via dehydration or dehydrogenation The second group consists of surface spectroscopies, such as photoelectron spectroscopy (PES) and high-resolution electron energy-loss spectroscopy (HREELS), which serve to characterize the intermediates leading to the gas-phase products The two classes of techniques are complementary and both are essential to build a complete understanding of the surface reactions General descriptions of these techniques can be found elsewhere [14,15]

In general, the application of these techniques (under the low pressure conditions of UHV) shows that HCOOH typically decomposes in two steps (1) the molecular acid reacts with the metal to produce a surface intermediate, (2) the intermediate may decompose to produce CO, CO_2, H_2O, H_2, atomic O or atomic C The first four products would typically be detected as gas-phase products, whereas the last two could remain as surface residues The first four products are the classical dehydration and dehydrogenation products, whereas the last two represent products of even more extensive decomposition The decomposition intermediate is usually identified as adsorbed formate, illustrated in Fig 1(a) in its various possible bonding configurations Some studies also postulate the anhydride and formyl intermediates shown in Fig 1(b) as products of bimolecular dehydration It should be noted that CO_2 is not typically stable on metal surfaces at temperatures above 80 K, so observation of CO_2 desorption is usually assumed to occur immediately upon its formation In other words, CO_2 evolution is "reaction-rate-limited" rather than "desorption-rate-limited" This is useful, since CO_2 evolution can then be taken to signify decomposition of the intermediate

In comparing results from the electrochemical studies with the surface science–UHV work, many differences must be taken into account These differences are so severe, in fact, that the validity of the comparison must itself be considered with great caution The differences include the following the solvent and associated ions (present in the electrochemical cell, usually absent in UHV), the applied potential and the electric field (controlled in the electrochemical cell, present in an analogous but less-controlled fashion in UHV), the reaction temperature (typically room temperature in the electrochemical cell, but varying widely in UHV) These differences have been discussed thoughtfully by several authors [16–22]

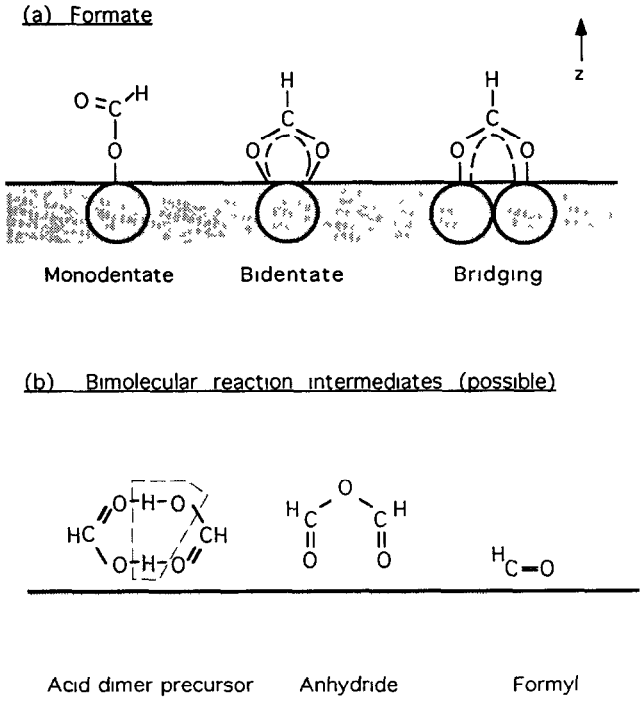

Fig 1 Structures of the surface intermediates most commonly postulated in decomposition of HCOOH on the group VIIIB transition metals (a) various forms of formate, (b) possible products of bimolecular dehydration—formic anhydride and formyl The acid dimer is a highly probable precursor

For the purposes of this review, it must especially be noted that the UHV experiments are usually carried out in such a way as to detect only majority reactions and their intermediates Minority species produced, for instance, at levels one or more orders of magnitude below that of the majority state would typically go unnoticed If the electrochemical poisoning intermediate forms at a rate much different from the reactive intermediate—which does not appear to be established from electrochemical studies—and if the two species form at similar rates in UHV, then the UHV studies would probably fail to identify the more slowly formed intermediate Minority states generated in UHV studies are often attributed to reactions at defect sites or at impurities, so do not receive much consideration, furthermore, minority states could easily be masked by majority states if present at relative concentrations less than about 10%, if probed by techniques such as PES or HREELS

The purpose of this article is not to judge the validity of the comparison between electrochemical and UHV surface science The purpose is simply to make the surface science literature more accessible to the electrochemical community, so that individual scientists may make their own comparisons and judg-

ments To that end, we review the adsorption and decomposition of HCOOH on various transition metal surfaces, studied in UHV

Madix reviewed this literature in 1980 for Cu, Fe, W, Ni, Ru and Ag [23] We include these metals, and also cover Pt, Au, Rh and Pd We first discuss molecular (non-dissociative) adsorption on all the metals in Section 2, then undertake a metal-by-metal survey of the decomposition reaction products and intermediates in Section 3 Section 4 is a critical summary of Section 3, providing a broad overview of the dissociative reaction pathways and comparing results for different metals In the course of reviewing the literature, we also point out instances where controversies or discrepancies might be resolved by re-interpretation, or might be the result of experimental artifacts

2. Molecular adsorption: All metals

Thermal desorption of molecular HCOOH has been measured for several metals Ag(110) [24], Au(110) [25], Cu(110) [26–28], Ni(111) [29], Ni(110) [30], Ni(100)–p(2 × 2)C [31], Pd(100) [32], Pd(111) [33], Pt(100) [34], Pt(111) [35–37], Rh(111) [38], Ru(001) [39] and Ru(100) [40] The majority of these studies [24,25,27,31,32,34,37–40] identify two states, one assigned to desorption from multilayers, and the other to desorption from a chemisorbed layer (The desorption temperatures reported for these two states vary, depending on the surface, from 145–190 K to 160–210 K, respectively Desorption states in this article are described by their peak temperatures only) In addition, some desorption of molecular HCOOH has been detected from Pt(111) [36] and Ni(110) [30] (230–250 K) following adsorption of HCOOH at 200 K, i e a temperature too high to populate the two states mentioned previously The origin of these high temperature states, relative to the states at 145–190 and 160–210 K, is not clear, although one possibility is that they result from the recombination of formate and atomic H, which has been shown to occur at 240–300 K on Pt(111) [41]

Details regarding the molecular orientation and bonding of the acid are available from PES measurements Various orientations of molecular HCOOH are shown in Fig 2 Joyner and Roberts used this technique to study the adsorption and decomposition of HCOOH on polycrystalline surfaces of Cu, Ni and Au [42] They proposed that molecular HCOOH adopts the same structure on all three metals following adsorption at 80 K, this structure consists of hydrogen-bonded chains of HCOOH, with the molecular plane parallel to the surface Such a structure (illustrated in Figs 2(c) and 2(d)) is very similar to that of solid-phase HCOOH [43–46] Heating the overlayer causes changes

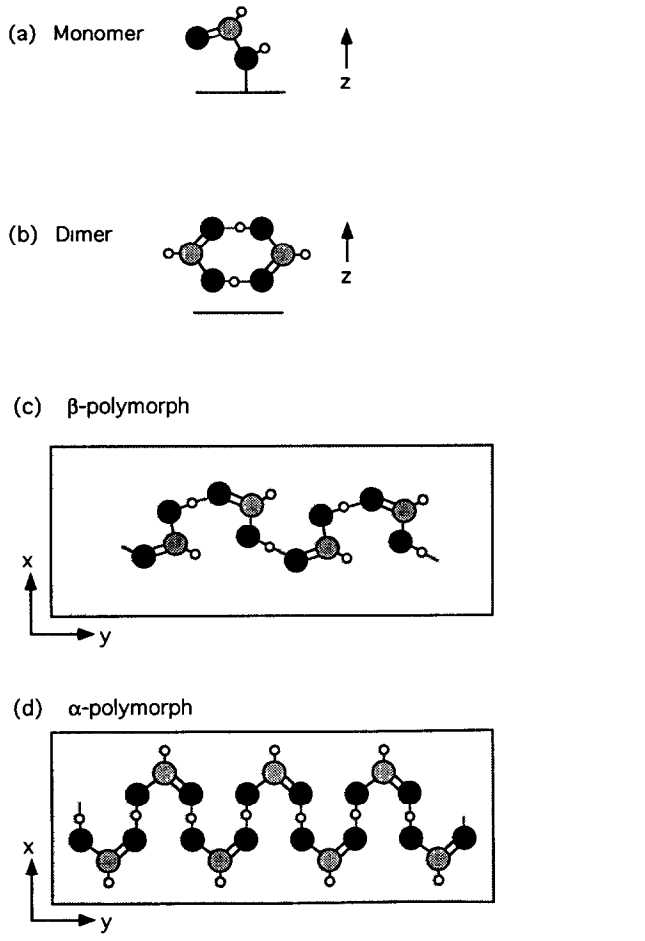

Fig 2 Commonly postulated structures of molecular HCOOH following adsorption on group VIII B transition metals (a) monomer, (b) dimer, (c) beta polymorph, (d) alpha polymorph, •, C, ○, O, ○, H The z axis is perpendicular to the surface plane, x and y axes lie in the plane

in the phototelectron spectra, which are assigned as follows (1) breakdown of the hydrogen-bonded chains (120–150 K), producing HCOOH monomers, (2) reorientation of the monomers relative to the surface plane (150–170 K), (3) loss of the hydroxyl proton (170–190 K) This agrees well with the Bowker and Madix interpretation of photoelectron spectra of HCOOH adsorbed on Cu(110) at 140 K [26], they identified HCOOH monomers bonded end-on through the hydroxyl O atom, as shown in Fig 2(a)

In addition to PES, vibrational spectroscopies have provided information pertaining to the configuration of molecular HCOOH A degree of randomness would be expected for the molecular orientation within multilayers and, indeed, a non-parallel orientation is found for HCOOH multilayers adsorbed on Cu(100) [47] and Ag(110) [24], based upon HREEL spectra Information is also available regarding the chemisorbed layer An

IR reflection–absorption spectroscopic (IRAS) study by Hayden et al [27] of HCOOH on Cu(11) revealed that HCOOH, which is in direct contact with the surface, does not have its molecular plane parallel to the surface and possibly forms dimer pairs (as shown in Fig 2(b)) For Pt(111), Avery used HREELS data to establish that multilayer acid adopts a hydrogen-bonded chain structure, with the molecular plane (at least nearly) parallel to the surface [35], this configuration exhibits vibrational features associated with the HCOOH solid state alpha polymorph [45] Columbia et al , also using HREELS, observed evidence for both the alpha and beta polymorphs, as well as dimer pairs for submonolayer HCOOH coverages on the same surface with a temperature- and coverage-dependent interconversion among these [48] Chtaib et al reported a dependence on the substrate geometry, with dimer pairs present on Au(111) and hydrogen-bonded chains on Au(110) [49], however, HREEL spectra for the (111) surfaces of Rh [50] and Pd [33] show the existence of hydrogen-bonded chains

3. Decomposition

3 1 Ni

Decomposition on the low-index surfaces of Ni yields products both of dehydration (CO, H_2O) and dehydrogenation (CO_2, H_2) Madix and coworkers have studied the interaction of HCOOH on clean Ni(110) and on Ni(110) covered with atomic C or O [13,30,51–57] They reported that HCOOH adsorbed on the clean surface at room temperature decomposes, resulting in the desorption of H_2O (320 K), followed by desorption of CO_2 and H_2 (390 K), and CO (390 K, 440 K), the ratio of the saturation desorption yields of CO to CO_2 is approximately unity [13] TDS experiments utilizing DCOOH identified the source of H_2O desorption as the hydroxyl groups [30], this suggests bimolecular dehydration Desorption of CO_2 and H_2 occurs over a very narrow temperature range [13], and accelerates during constant temperature experiments [52] Thus, Madix and coworkers concluded this decomposition to be autocatalytic They proposed that attractive interactions between the intermediates produce densely packed islands on the surface, decomposition of one adspecies immediately destabilizes neighboring adspecies, producing a chain reaction [53] The decomposition also left CO on the surface, affording additional CO desorption (440 K)

Adsorption at lower temperatures (about 200 K) diminishes the autocatalytic behavior, broadening and decreasing the temperature range of decomposition [30] Presumably, this is because island formation is inhibited by low temperature adsorption The presence of a surface carbide results in less CO desorption and decomposition over a higher, broader temperature range [51,54,55] The coadsorption of O enhances the yield of CO_2 [57]

The (100) face of Ni decomposes HCOOH in a manner similar to that Ni(110) [31,58] On the (100) surface, H_2O desorbs at temperatures about 100 K lower than those on the (110) surface, while the desorption temperatures of the other decomposition products do not shift significantly, however, the desorption features are not as sharp as those from the (110) surface [58] Benziger and Madix attributed this to diminished attractive interaction between the decomposition intermediate, induced by different substrate geometries [58] Decomposition also oxidizes the surface The presence of surface carbides also produces a marked decrease in the amounts of CO_2 and H_2 desorbed [31]

The identification of the decomposition intermediate has been somewhat controversial on Ni Madix and coworkers originally proposed that the intermediate is formic anhydride, shown in Fig 1(b) They associated the autocatalytic behavior with the existence of the anhydride This intermediate (formic anhydride) could result from the dehydration of the acid dimer and could decompose further, according to the reaction (see Fig 1(b))

$$\underset{\text{acid dimer}}{2(HCOOH)} \rightarrow \underset{\text{anhydride}}{H_2C_2O_3} + H_2O \rightarrow \underset{\text{formate}}{HCO} + \underset{\text{formate}}{HCOO}$$
$$\rightarrow H + CO + \underset{\text{formate}}{HCOO} \rightarrow CO + CO_2 + H_2 \qquad (1)$$

The proposition of anhydride as an intermediate in surface catalysis was based partly on the simultaneity of CO_2, H_2, and CO desorption, partly on the relative yields of CO and CO_2 (about 1 1), and partly on the observation that H_2O is produced by bimolecular dehydration, all of which are consistent with reaction (1) —but which do not uniquely identify that reaction According to their interpretation, neither formyl nor formate would be a stable surface intermediate, instead, the anhydride would be stable right up to the point of CO, CO_2 and H_2 desorption

Vibrational spectroscopy later suggested re-interpretation [59,60] Madix et al probed the intermediate on Ni(110) using HREELS, and observed the presence of coadsorbed CO and symmetrically bonded formate [61] This suggests that bimolecular dehydration produces formate and formyl—as in reaction (1)—followed almost immediately by decomposition of the formyl to CO and atomic H [61] Presumably, a similar mechanism could also account for the product distribution on other low-index faces (The anhydride may still

be a reaction intermediate, as shown in Fig 1, though a short-lived one and not stable up to the point of evolution of CO, CO_2 and H_2 gas, as originally suggested) Jones and coworkers, using HREELS and low energy electron diffraction (LEED), observed formate on Ni(110) in an ordered $c(2 \times 2)$ overlayer, they also determined the formate to be bonded in a "bridging" configuration (see Fig 1) [62,63] However, the possibility of formic anhydride as a surface intermediate—at least on Ni(111)— has been recently resurrected, based on IRAS [29] The validity of this conclusion is discussed in more detail in Section 3

Benziger and Schoofs also pointed out that the gas-phase HCOOH monomer or dimer composition can have a strong effect on the surface decomposition on Ni(111) [64] For vapor dominated by HCOOH dimers, decomposition closely follows the autocatalytic behavior attributed originally to formic anhydride, with the production of both CO and CO_2 This implies, somewhat surprisingly, that the gas-phase dimer remains intact upon adsorption However, for vapor consisting primarily of monomers, decomposition yields primarily CO_2 Presumably, the CO_2 results from unimolecular deprotonation of the acid to formate, followed by further unimolecular deprotonation

$$HCOOH \rightarrow HCOO + H \rightarrow CO_2 + 2H \quad (2)$$

Erley and Sander also reported autocatalytic behavior following the adsorption of formic acid dimers on the same surface [29], as well as the desorption of H_2O (235 K) In many other experimental studies, the gas-phase monomer or dimer composition has been an unrecognized and uncontrolled variable This may contribute to the confusion which has surrounded the discussion of surface intermediate(s), especially on Ni

3 2 *Ru*

Larson and Dickinson have studied HCOOH decomposition on Ru(100), utilizing thermal desorption [40], desorption of H_2O (183–220 K), H_2 (390 K), CO_2 (390 K) and CO (488 K) are observed The H_2O peak desorption temperature decreases with increasing HCOOH exposure, suggesting a second-order dehydration similar to that for Ni, also, a CO/CO_2 ratio of unity is observed, Unlike Ni, however, no autocatalytic behavior is reported

Avery and coworkers identified bridging formate as the decomposition intermediate on Ru(001), using HREELS [59,60] They also identified losses caused by the presence of CO, similar to the HREEL spectra for Ni(110) [61], the intensities of these losses increase with the surface temperature as the intensities of the formate losses decrease This implies that the decomposition of formate produces CO, in contrast to reaction (1) and unlike any mechanism discussed thus far

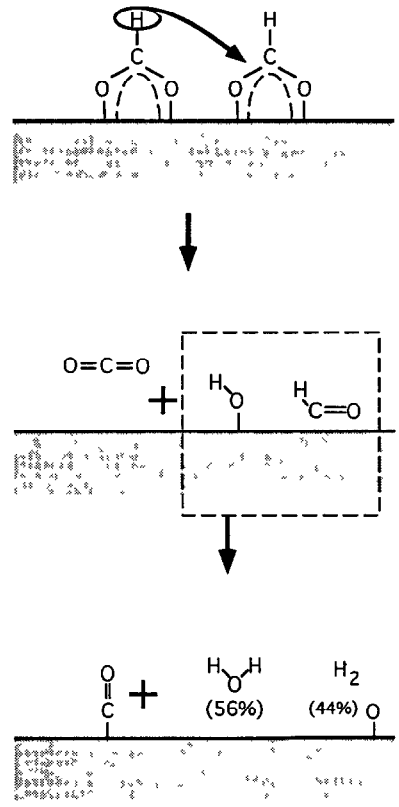

Fig 3 Reaction model for bimolecular decomposition of formate on Ru(001), as proposed by Sun and Weinberg [39]

Sun and Weinberg reported the same desorption products from the (001) surface as those from the (100) surface, as well as a CO/CO_2 ratio of unity [39], however, the (001) surface displays autocatalytic behavior with CO_2 desorption features exhibiting narrower full width at half-maximum (FWHM) and higher peak desorption temperatures (from 330 K at onset to 395 K at saturation) The desorptions of H_2 (resulting from the acyl proton) and H_2O also follow this trend The desorption of H_2 (resulting from the hydroxyl proton) occurs at lower temperatures (320 K) and is clearly discernible at saturation CO desorbs in a single state above 400 K Sun and Weinberg proposed the "hot hydrogen" decomposition mechanism illustrated in Fig 3, which is based on the formate intermediate, such that

$$2HCOOH \rightarrow 2HCOO + 2H \rightarrow 2HCOO \rightarrow CO_2 + CO + H_2O + H_2 \quad (3a)$$

$$\text{or} \rightarrow CO_2 + CO + O + 2H_2 \quad (3b)$$

In this model, decomposition of one formate adspecies via C–H bond cleavage produces a "hot" H

atom, which inserts itself between the C and O atoms of a neighboring formate This ruptures a C–O bond, producing CO as well as adsorbed hydroxyl, H and O (Note that both reactions (3a) and (3b) occur on Ru(001) This produces desorption of CO_2, H_2 and H_2O between 330 K and 395 K, desorption-limited CO above 400 K, and a small amount of atomic O which does not desorb It is important to note that, according to this mechanism, H_2O cannot be produced before CO_2 (assuming, as discussed in Section 1, that evolution of gaseous CO_2 occurs as soon as formate decomposes) In this model, the increasing temperature of the autocatalytic desorption is explained by attractive interactions between the formate adspecies

3 3 Cu

CO_2 and H_2 are the only desorption products resulting from HCOOH exposure to clean Cu(110) at temperatures above 200 K [26,27,65] H_2 desorbs in a broad state, (270–280 K) and a narrower state (450–475 K), CO_2 desorption also peaks at 450–475 K, and the peak shape is identical to the higher temperature H_2 desorption feature The simultaneous desorption of CO_2 and H_2 is attributed to the decomposition of a formate intermediate The use of DCOOH reveals that low temperature H_2 desorption results from H atoms produced when the molecular acid loses the hydroxyl proton, however, the desorption temperature is 50 K lower than that for H_2 desorption from H adatoms on clean Cu(110) [26,65] A possible reason for this is site blocking by the coadsorbed formate, which forces H adatoms out of the preferred adsorption sites [26] Similar desorption occurs from Cu(100), with the exception of the low temperature H_2 feature, which appears much closer to the peak temperature for H_2 desorption from the clean surface [66]

The coadsorption of atomic O with HCOOH on the (110) face increases the amount of formate intermediate produced and suppresses the low temperature H_2 desorption This is attributed to the consumption of the acidic proton by the O adatoms to form H_2O, with hydroxyl as a possible intermediate, according to [26,28]

$$2HCOOH + O \rightarrow HCOOH + HCOO + OH \rightarrow 2HCOO + H_2O \quad (4)$$

Coadsorbed C atoms accelerate the decomposition of formate, as well as forming a surface carbonate with the formate fragments at higher C coverages [28]

Sexton confirmed formate as the decomposition intermediate on Cu(100), using HREELS [47,67] The adspecies produced following the adsorption of several layers of HCOOH at 100 K and subsequent heating to 400 K possess the bridging configuration (This agrees with photoelectron spectroscopic results showing the formate O atoms to be equivalent [26])

On the (100) face, Sexton proposed that cooling to 100 K lowers the symmetry of the formate, possibly as a result of the adoption of non-equivalent binding sites for the formate O atoms [47] Hayden et al , utilizing IRAS, observed bridging formate on Cu(110), following HCOOH adsorption at 100 K and heating to 290 K, however, no temperature-dependent symmetry degradation was reported to occur as on the (100) surface Nevertheless, the phenomenon was observed following exposure of the annealed overlayer to additional HCOOH [27,68] Dubois et al also failed to reproduce Sexton's results on Cu(100) and, as on Cu(110), observed symmetry degradation only after exposing a formate overlayer to additional HCOOH [66] They concluded that the symmetry degradation results from tilting of the formate, caused by hydrogen bonding to molecular HCOOH This may have occurred inadvertently in Sexton's original experiment as a result of the re-adsorption of molecular acid from background gas upon cooling to 100 K

Detailed bonding geometries have been proposed for formate on Cu surfaces on the basis of techniques other than HREELS, however, the results for the (100) surface are very controversial Surface extended (SEXAFS) and near-edge X-ray analysis of fine structure (NEXAFS) indicate that formate is situated with its O atoms located near the fourfold hollow sites, and that the Cu–O bond distance is 2 3–2 4 Å, which is at least 0 3 Å longer than expected from bulk Cu formate [69,70] Newer data from photoelectron diffraction (PHD), coupled with re-analysis of the SEXAFS and NEXAFS data, suggest that the Cu–O bond distance is about 2 Å, with the O atoms pointing toward next-nearest-neighbors ("diagonal" fourfold hollows) [71,72]

A "normal" Cu–O bond distance was also arrived at by Woodruff et al , but a third adsorption site is also proposed, i e with the formate O atoms located in nearest-neighbor, on-top sites rather than fourfold hollow sites [73] This last result is also supported by a theoretical calculation [74] A PHD study by Caputi et al ruled out the second (diagonal) adsorption geometry but is consistent with the other two [75] Of the three configurations proposed, only the third conforms to the "bridging" geometry derived from HREELS data and illustrated in Fig 1(a) Thus, the details of formate's adsorption geometry on Cu(100) still appear to be unresolved, despite the battery of powerful techniques which have been brought to bear On Cu(110), Puschmann and coworkers determined that formate is adsorbed with the O–C–O plane parallel to the Cu atom rows, and with the O atoms sitting nearly on top of adjacent atoms in a row (the bridging configuration

of Fig 1(a)) This positioning permits a Cu–O bond distance identical to the bulk Cu formate value [76,77], which is consistent with the more recent data for Cu(100)

3 4 Pt

Thermal desorption results reported for the low-index faces of Pt vary greatly Kizhakevariam and Stuve observed no decomposition products from clean Pt(100), but did observe desorption of CO_2 (310 K) and H_2O (180 K, 310 K) from a Pt(100) surface predosed with atomic O [34] Madix reported desorption of D_2O, H_2O, D_2, H_2, CO and CO_2 from Pt(110) exposed to DCOOH at 200 K, with only the peak desorption temperature of CO_2 reported (260 K) [23] On Pt(111), Abbas and Madix reported desorption of CO_2 (265 K, 361 K, 426 K), H_2O, D_2O and HDO (265 K, 295 K), H_2, D_2 and HD (310–320 K), and CO (473 K, 531 K) from exposure to DCOOH at 195 K, at saturation, the majority products are CO_2 and the hydrogenic species, leading to the assignment of CO and the aqueous species to reactions at surface defect sites [36] Avery [35] and Columbia and Thiel [37] reported only CO_2 (260 K) and H_2 (360–370 K) as desorption products following adsorption of HCOOH at 130 K or below, any CO desorption is ascribed to ambient adsorption These reports contrast with the observations of Seebauer *et al*, who found CO and H_2O as the majority products, with a CO/CO_2 ratio of two [78] (A possible explanation for the large amounts of CO reported by Seebauer *et al* is the use of background dosing as the method of exposing their surface to HCOOH In our own work, we have observed large increases in the residual background pressures of CO and H_2O in a vacuum chamber when this exposure technique is used in place of a directed gas beam The direct gas beam approach is generally preferred for gases, such as HCOOH, which may react strongly with chamber walls) A unimolecular dehydrogenation mechanism, as shown in reaction (2), thus seems most likely for Pt(111)

The reactivities of Pt(111) and Pt(100)-hex seem different at first glance, decomposition being observed for Pt(111) but not for Pt(100) However, the absolute yield of CO_2 and H_2 on Pt(111) is estimated at only 0 05–0 1 monolayers [37] This is a small amount and so, in a quantitative sense, the behavior of the two surfaces may not be so different after all Considering that its chemistry also seems much less complex than that of others, such as Ni or Ru, Pt may be categorized as a rather unreactive metal toward HCOOH decomposition

HREEL spectra reveal bridging formate to be the intermediate on Pt(110) and Pt(111) [35,48,79,80]—again consistent with reaction (2) Additionally, Avery reported the existence of monodentate formate on oxygen-predosed Pt(111) for submonolayer doses of HCOOH at 130 K [80], he observed the conversion from this to the bridging configuration over a period of 20 min Columbia et al also observed a mixture of monodentate and bridging formate on the same surface, but only for exposures made at 80–100 K, heating to 120 K was sufficient to cause complete conversion to the bridging form [48]

Coadsorbates have also been studied on Pt surfaces As mentioned above, atomic O induces HCOOH decomposition on Pt(100) [34], it increases the extent of decomposition on Pt(111) by a factor of 4–7, as well as producing H_2O, in addition to CO_2 and H_2 [35,81] Atomic H suppresses decomposition, as would be expected from reaction (2) [82] The presence of coadsorbed S suppresses any CO and H_2O produced by decomposition, presumably by preferentially adsorbing at defect sites [36] The deliberate introduction of CO (a suggested poison in electrochemical oxidation) suppresses decomposition, probably by blocking sites necessary for deprotonation [83]

3 5 Pd

The (100) face of Pd is unusual in two respects First, decomposition of HCOOH appears to follow neither dehydration nor dehydrogenation pathways, instead, CO and H_2 are the two main reaction products Secondly, surface spectroscopies fail to identify any stable reaction intermediate These generalizations are based upon three major studies reported in the literature, by Jorgensen and Madix [84], Sander and Erley [85], and Solymosi and Kovacs [32]

Jorgensen and Madix reported that the only desorption products are molecular acid (180 K) and CO (515 K), following HCOOH adsorption at 80 K They verified this with HREELS, which identifies vibrations associated with molecular HCOOH prior to its desorption, a CO loss appears and remains the only loss after molecular desorption is complete [84] Solymosi and Kovacs also observed H_2 and small amounts of H_2O as desorption products, but their spectroscopic evidence indicated no intermediate as being present Sander and Erley reported desorption of small quantities of CO_2 and H_2O (180 K), and larger amounts of H_2 (330–350 K) and CO (480 K), with respect to intermediates, however, their FTIR spectra revealed only molecular HCOOH vibrations prior to heating to 170 K, and only a CO vibration after heating to 190 K No vibrations were observed which might signal formate or formic anhydride [85]

Jorgensen and Madix observed the presence of formate on an oxygen-predosed Pd(100) surface, which produces CO_2 desorption (265 K) upon decomposition

[84], Solymosi and Kovacs reported similar results for K coadsorption Formate is also identified by PES on Pd(100) covered with Na adatoms [86] The fact that coadsorbates can stabilize formate suggest that it also may be a short-lived intermediate on the clean surface On balance, it appears that the overall reaction for the clean (100) face must be written as [32]

$$HCOOH \rightarrow CO + H_2 + O \quad (5)$$

In support of this, some authors have reported that residual O remains on a Pd(100) surface after desorption of all gas-phase products [32,85]

The (111) face of Pd is less remarkable Davis and Barteau observed the desorption of CO_2 (260 K), H_2 (330 K) and CO (490 K), the CO/CO_2 ratio is 0 3–0 5 [33] Their HREEL spectra identified formate as the intermediate, with decomposition products CO and CO_2, and atomic O and H The addition of O adatoms to this surface results in the conversion of all the adsorbed acid to formate, with the addition of H_2O as a desorption product (220 K, 280 K)

3 6 Rh

Solymosi et al have studied the decomposition of HCOOH on Rh(111) using TDS, AES, PES and electron energy loss (EEL) [38,87,88], Houtman and Barteau have also studied this system using HREELS and TDS [50] Solymosi et al reported that the adsorption of HCOOH at 100 K produces desorption of CO_2 (two states, 230–255 K and 262–290 K), H_2 (323–358 K), H_2O (251–263 K) and CO (530–537 K) Saturation levels for CO and H_2O are attained at exposures 20%–25% of those needed to saturate CO_2 and H_2 desorption, the saturation CO/CO_2 ratio is 0 3 PES and EEL spectroscopy identified the presence of formate above 150 K, above 240 K, formate disappears and CO emerges, reminiscent of the results for Ru(001) Two formate decomposition reactions are proposed to explain these observations the majority reaction involves breaking the formate C–H bond, resulting in CO_2 desorption and H adatoms, while the minority reaction relies on the rupture of a formate C–O bond, this produces CO admolecules, and H and O adatoms, which can combine to produce H_2O

It is possible that this minority reaction involves a hot hydrogen mechanism, such as that proposed for Ru(001) [39] The presence of both atomic O and atomic K enhances the initial dehydrogenation of molecular HCOOH and increases the amount of formate produced Houton and Barteau agreed fundamentally with the TDS results reported by Solymosi et al , and gave support to the basic decomposition mechanism proposed, on the basis of their vibrational spectra

3 7 Ag and Au

HCOOH has not been observed to decompose on clean Ag, coadsorbed O is needed to initiate deprotonation and produce formate [24,89] Barteau et al reported the desorption of H_2 and CO_2 (410 K), following adsorption of HCOOH by an oxygen-dosed Ag(110) surface at 300 K, a small amount of molecular HCOOH desorption accompanies this, with H_2O desorption occurring immediately upon adsorption at this temperature [89] HCOOH adsorption at 100 K allows the observation of this desorption (200–210 K) [24], which originates from deprotonation of HCOOH by atomic O, the subsequent CO_2 and H_2 result from formate decomposition

Sexton and Madix have used HREELS to identify formate as the adsorbed intermediate produced by the reaction between atomic O and molecular HCOOH on Ag(110) [24] The formate produced following adsorption of HCOOH at 100 K and heating to 175 K exhibits a monodentate configuration An irreversible conversion to a bridging configuration results from heating the overlayer above 300 K, this is similar to the behavior observed on Cu(100), where the conversion was reported to be reversible [47] This conversion also possesses a coverage dependence, with the bridging configuration observed exclusively at low HCOOH exposures Increasing exposure results in the predominance of the monodentate configuration, which is explained by surface crowding caused by coadsorbed H_2O Heating to 300 K desorbs H_2O and provides enough energy to reorient the formate NEXAFS studies showed that the orientation of formate on Ag(110) differs from that on Cu(110), with indications of a molecular plane tilt away from the surface normal and a lack of azimuthal alignment [90]

Outka and Madix reported no decomposition from clean Au(110) but observed it on the O-covered surface, as on Ag(110) (This also agrees well with studies of formaldehyde [25] and methanol [91] on Au(110) by the same authors) They reported the desorption of H_2O (T_p = 200 K, 340 K) and CO_2 (340 K), molecular desorption accompanied the desorption features at 340 K but no H_2 desorption was observed, as on Ag(110)

Chtaib et al reported the desorption of CO_2 and H_2 (180 K) following adsorption of HCOOH on polycrystalline Au [92] They also detected formate after heating an adlayer of HCOOH above 170 K, by monitoring the C and O XPS spectra, these spectra exhibited changes similar to those reported by Joyner and Roberts, caused by the reaction of HCOOH with films of Au, Cu and Ni [42]

Chtaib et al also reported HREEL studies for HCOOH decomposition on Au single crystals [93] They observed no evidence for the presence of formate

on the (110) surface after heating the overlayer to temperatures as high as 500 K, but did see loss features indicative of O adatoms at this temperature On the (110) face, the existence of formic anhydride was posited, based on the loss spectrum produced after the HCOOH overlayer was heated to 245 K This loss spectrum differs markedly from the HREEL and IR spectra reported by Erley and Sander for formic anhydride on Ni(111) [29] These differences are compared in Section 4

Comparing the data available for Au, there appears to be disagreement over whether HCOOH decomposes on this metal Qualitatively, this parallels the disagreement which developed in the early 1980s over whether molecular O_2 adsorbs on Au The O_2 controversy was apparently resolved by the discovery that Si contamination can initiate adsorption of O_2 [94] (In its oxidized form, Si is difficult to distinguish from Au by the technique used most commonly to ascertain surface cleanliness, i e Auger electron spectroscopy [95]) It is possible that contamination plays a similar role in the reports of HCOOH decomposition, at least in those reports which pre-date the discovery that Si can alter significantly the chemical reactivity of this metal

3 8 W and Fe

Benziger and Madix have studied the reaction of HCOOH with Fe(100), using TDS and X-ray photoelectron spectroscopy (XPS) [96,97] They observed the simultaneous desorption of CO, CO_2 and H_2 (490 K) following adsorption of HCOOH at 160 K, additional desorption states for H_2 (350 K) and CO (800 K) are reported XPS identifies a symmetrically bonded formate as the reaction intermediate, following loss of the molecular acid's hydroxyl proton This produces H adatoms which desorb as H_2 (350 K) Formate decomposes above 400 K, resulting in the simultaneous desorption of CO, CO_2 and H_2 This decomposition also yields O and C adatoms, which combine and desorb as CO above 700 K The CO/CO_2 ratio at saturation is slightly less than unity

Benziger *et al* found W to be extremely vigorous in its decomposition of HCOOH [98] The only desorption product they observed following low HCOOH exposures (less than 0 7 l) on W(100) at 300 K and subsequent heating to 800 K was H_2, Auger electron spectroscopy identified the surface to be covered by O and C adatoms following this desorption For higher exposures, the simultaneous desorption of CO_2, H_2 and H_2O occurs (580 K), this desorption is attributed to the decomposition of a formate species The build-up of adatoms on the surface diminishes its ability to dissociate completely the molecular acid, resulting in the production of formate This is confirmed by the production of formate at lower HCOOH exposures on a W(100)–(5 × 1)C surface Bhattacharya suggested molecular formaldehyde and formyl, in addition to formate, as possible reaction intermediates on clean W(100), based on PES [99], although the use of a vibrational spectroscopy would be far more definitive in this regard

4. Discussion of dissociative reaction pathways

As mentioned in the Introduction, HCOOH generally reacts with a transition metal in three identifiable steps molecular adsorption, reaction of the molecular acid to form a surface intermediate, and decomposition of this intermediate Molecular HCOOH adsorbs in configurations which resemble its solid-phase (hydrogen-bonded chains) and gas-phase (dimer pairs) forms The molecular acid is then dehydrated or dehydrogenated by the metal, on more inert metals, such as Ag and Au, this step occurs only in the presence of coadsorbed atomic O On other metals, such as Pt and Cu, this step is enhanced by the presence of coadsorbed atomic O We now turn our attention to the stable intermediates which may result from dehydrogenation and dehydration, much of our discussion will be centered around the flow chart in Fig 4, where the dark

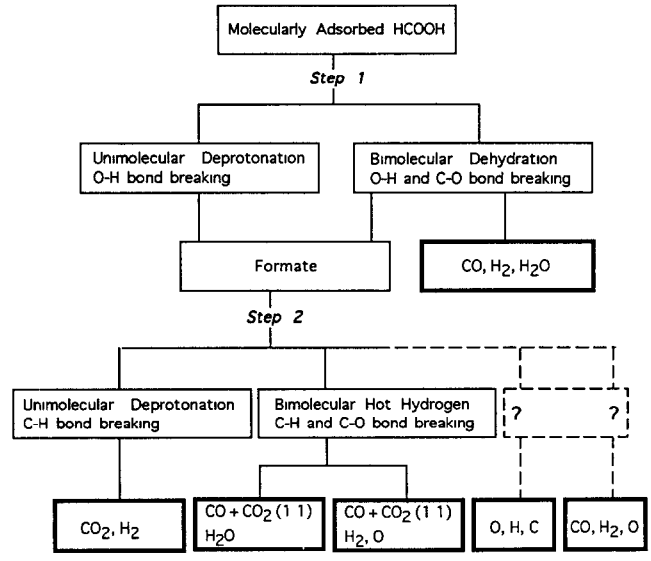

Fig 4 Flow chart, illustrating pathways by which the formate intermediate can form and decompose Dark boxes show the end products of the reactions observed in UHV studies Dashed lines illustrate pathways which are speculative and which concern the two surfaces categorized as "most reactive" in Table 1 Pd(100) and W(100) Stoichiometry cannot be taken directly from Fig 4, except for the fact that formate decomposition via bimolecular hot hydrogen insertion yields a 1 1 ratio of CO to CO_2

boxes show the observable end products of decomposition in vacuum It should be noted that the products of bimolecular dehydration necessarily include CO, H_2 and H_2O

Formate is the only species identified on Cu, Pt, Ru, Pd, Rh, Ag, Fe and Ni(110) by vibrational and photoelectron spectroscopies On W, formate, formaldehyde and formyl have all been suggested, based on PES, although no definitive selection was made However, formaldehyde and formyl should both give rise to CO, in contrast to the observation that CO_2 is the only C-containing product which desorbs from this metal This supports formate as the most reasonable intermediate of these three

On Au(111) and Ni(111), formic anhydride has been reported as a stable intermediate, on the basis of vibrational spectroscopies, but we find both assignments to be questionable The vibrational spectra for anhydride on these two surfaces are markedly different Turning first to Ni(111), the HREEL spectra exhibit all the same features present in HREEL spectra of bridging formate on many other surfaces The identification of anhydride on Ni(111) is based partially upon the identification of two C–H stretching modes with IRAS (which affords resolution superior to that with HREELS) Sander and Erley took this as evidence of an intermediate with two types of H atom, namely formic anhydride (see Fig 1) This conclusion contradicts the work of Hayden et al , which identified two vibrational features in the same frequency region (2900–3000 cm^{-1}), according to IR spectroscopy of formate on Cu(110) [27,68], one of these features is assigned to the C–H stretch, while the second is assigned to a combination of two other vibrations within the formate intermediate The existence of formate (rather than anhydride) on Cu(110) seems quite well

TABLE 1 Categorization of metals with respect to reactivity for HCOOH decomposition, based upon the reactions by which the formate intermediate forms and decomposes

Metal	Step 1 formation of the formate intermediate	Step 2 decomposition of the formate intermediate	Ref
Unreactive	None		
Ag(110)			24, 89
Au(110)			91
Pt(100)			34
Slightly reactive	Unimolecular dehydrogenation	Unimolecular dehydrogenation	
Cu(100), (110)	(= deprotonation)		26, 27, 65, 66
Pt(111)			35, 36, 48
Moderately reactive	Unimolecular dehydrogenation	Mixture unimolecular dehydrogenation +	
Pd(111)		bimolecular hot hydrogen	33
Rh(111)			38, 87, 88
Fe(100)			96, 97
Very reactive I	Dehydrogenation	Bimolecular hot hydrogen	
Ru(001)			39, 59
Very reactive II	Bimolecular dehydration [a]	Unimolecular dehydrogenation [a]	
Ru(100)			40
Ni(111), (100), (110)			13, 29, 30, 52, 53, 56, 58, 64
Most reactive	{Dehydrogenation?}	?	
Pd(100)			32, 84, 85
W(100)			98

A high reactivity corresponds roughly to a high degree of complexity and diversity in the reaction products or (in the case of the "most reactive" metals) to a decreasing degree of molecularity Figure 4 illustrates the possible reactions and their products in detail In some cases, we have re-interpreted the original authors' conclusions, based upon reasoning outlined in the text In particular, the idea that the results for the "moderately active" metals might involve a hot hydrogen mechanism is our own, the hot hydrogen mechanism was proposed after these papers were published, although the original authors did posit that C–O bond cleavage must be involved Note that we have been somewhat critical in selecting references to include to support these mechanisms, i e the reference lists are not comprehensive

[a] For Ni(111), there is evidence that bimolecular dehydration prevails as Step 1, and unimolecular dehydrogenation as Step 2, if the gas-phase acid is dimeric (The yield of CO CO_2 is about unity [64], the CO_2 desorption kinetics appear to reflect distinctive autocatalytic behavior [29,64], and H_2O evolves at low temperature [29]) However, when the gas-phase starting material is monomeric, the data available are insufficient to determine the mechanisms of Step 1 and Step 2 (The yield of CO CO_2 is about 0 3 [64], but no information on low-temperature water desorption is available)

established, both on spectroscopic grounds and by the absence of CO desorption (As shown by Fig 4, bimolecular dehydration necessarily forms CO) Thus, the Cu(110) work indicates that the observation of two vibrational modes in the C–H stretching region does not provide firm evidence for anhydride rather than formate This in turn casts doubt on the existence of anhydride as the intermediate present on Ni(111) Other IR experiments which Erley and Sander reported utilizing DCOOH also support the existence of the anhydride, however, control experiments are not described which would ascertain that the spectra are different for surfaces where formate—not anhydride—is clearly established Such experiments would be necessary to establish the basis of the anhydride assignment on Ni(111)

The HREEL spectra of formic anhydride on Au(111) present a number of inconsistencies (1) no Au–O vibrations are observed in the spectrum, regardless of the anhydride's orientation, this vibrational mode should be present in the HREEL spectrum, based on the selection rules for the technique, (2) the fingerprint vibrations, i e the symmetric and asymmetric C=O stretching modes, are not sufficiently resolved by the HREEL technique to confirm the existence of anhydride, (3) the spectra reported are obtained after heating the Au crystal to 245 K, which is 65 K above the maximum reported temperature for H_2 and CO_2 desorption from HCOOH decomposition on polycrystalline Au In addition, no CO desorption has been reported from the decomposition of HCOOH on Au, this would be expected if anhydride were present (see Fig 4)

In light of the above discussion, we believe formate to be the only stable intermediate formed on the metal surfaces presented in this review We turn next to the mechanisms by which this intermediate may form and may subsequently decompose The majority of the evidence useful in deducing these pathways comes from TDS

In Table 1, we attempt to summarize the decomposition reactions (steps 1 and 2 of Fig 4) catalyzed by various metals In some cases, we reinterpret the data or extend their original interpretation in light of later developments We use several criteria to decide which reactions are catalyzed by the metals Starting with step 1, the flow chart in Fig 4 shows that some products of bimolecular dehydration (CO, H_2, H_2O) will form before the formate intermediate decomposes, assuming step wise decomposition Of these products, H_2O typically has the lowest adsorption energy and should desorb at relatively low temperatures (Molecular H_2O is not stable on clean metal surfaces above 300 K [100]) Furthermore, when the formate intermediate later decomposes, it must produce some CO_2, as mentioned in Section 1, the desorption of CO_2 will occur simultaneously with formate decomposition Therefore, the desorption of H_2O at temperatures below those of CO, H_2 and CO_2 indicates dehydration as step 1, dehydration also must produce CO (eventually) as a decomposition product In contrast, the absence of low temperature H_2O and CO as desorption products signals unimolecular deprotonation as the first step to decomposition in Fig 4 Other evidence of bimolecular dehydration, such as isotopic labeling of the hydroxyl protons, is also valuable

The next choice is to identify the route by which the formate intermediate breaks down (step 2) Here, knowledge of the CO/CO_2 yield ratio can again be useful Let us consider first the case where step 1 is unimolecular deprotonation Then, if CO_2 and H_2 are the only decomposition products, the CO/CO_2 ratio is 0 and step 2 must be the unimolecular loss of the acyl H, with the overall reaction given by reaction (2) If CO is also produced, then a ratio of unity indicates the hot hydrogen mechanism as step 2, and the overall reaction is given by reaction (3) A lower ratio can be explained by a mixture of unimolecular deprotonation and bimolecular hot hydrogen Let us consider next the case where step 1 is bimolecular dehydration Here, the CO/CO_2 yield ratio can only be unity if step 2 is exclusively unimolecular deprotonation, and the overall reaction is given by reaction (1) Higher ratios (up to 3) can be obtained if any (all) of the formate reacts via hydrogen insertion A further criterion for assigning step 2 is that the hot hydrogen mechanism should always produce high temperature H_2O (at or close to the temperature for CO_2 desorption) and/or generate residual atomic O

It should be noted that the observation of CO alone cannot be used to identify both steps 1 and 2, one must somehow distinguish whether CO is formed via bimolecular dehydration or via the hot hydrogen insertion model For this reason, Sun and Weinberg went to great lengths to determine that all CO produced on the Ru(001) surface originated from the decomposition of formate and not from dehydration of the molecular HCOOH, this was a key justification of the hot hydrogen mechanism for that surface It is also interesting to note that, while the Ni surfaces exhibit a complex product distribution in many ways similar to that of Ru(001), there is good evidence that the Ni surfaces catalyze bimolecular dehydration as step 1 At the same time, the CO/CO_2 ratio is unity, indicating that the formate must decompose exclusively by C–H bond breaking In other words, despite many qualitative similarities, the chemistry on Ni faces appears to be fundamentally different from that on Ru(001)

Based upon the criteria described above, we make the mechanistic assignments shown in Table 1 The most severe re-interpretation of original authors' conclusions concerns Rh(111), Pd(111) and Fe(100), where we posit that formate decomposition proceeds via a mixture of simple C–H bond cleavage and the hot hydrogen model Whereas the original authors recognized that C–O bond breaking must be involved, the bimolecular insertion model was not yet available to explain it in more detail Decomposition on Pd(111) and Fe(100) does not produce any H_2O but does produce atomic O These two surfaces also display CO/CO_2 ratios less than unity, indicating that not all C–H bond ruptures result in a corresponding C–O bond being broken On Rh(111), two CO_2 desorption states apparently result from the two distinct pathways decomposition via the hot hydrogen path with a peak rate at 235 K, and simple C–H bond cleavage of the remaining formate, with a peak rate at 275 K

Finally, in Table 1, we have grouped the metals according to their degree of reactivity in HCOOH decomposition Except for the last category, we gauge "reactivity' by the diversity of reaction products By this criterion, the least reactive metals are Au, Ag and one face of Pt, which do not catalyze the decomposition of the acid For Au and Ag, this categorization is consistent with the low activity of these metals for other adsorbates in general The slightly reactive surfaces produce CO_2 and H_2 as exclusive desorption products, indicating unimolecular deprotonation for both steps 1 and 2 The moderately active metals are similar but, in addition, exhibit evidence for some bimolecular hot hydrogen insertion in step 2 The very active metals, i e Ru and Ni, exhibit complex behavior which has been discussed fully The category identified as "most reactive" is one for which the reaction products do not fit any simple reaction scheme, and for which a reaction intermediate has not been identified except after surface modification W apparently completely reduces the acid to its atomic constituents, which is consistent with the high activity of this metal for other adsorbates, and presumably results from its high affinity for C and O

5. Summarizing remarks

We have reviewed the literature which described studies of HCOOH acid reactions on metal surfaces in UHV At low temperatures, molecular HCOOH adsorbs in configurations which resemble its solid-phase (hydrogen-bonded chains) and gas-phase (dimer pairs) forms The molecular acid can then be dehydrated or dehydrogenated (deprotonated) by the metal, decomposition of the acid can be enhanced (or even instigated) by coadsorbed atomic O, presumably because the O has an affinity for the hydroxyl proton of the acid The only stable intermediate firmly identified as a result of the acid's decomposition is formate, although formic anhydride and formyl have also been suggested The formate itself can then decompose via one of two mechanisms unimolecular deprotonation (loss of the acyl H) or bimolecular hot hydrogen insertion These mechanisms can be distinguished largely upon the basis of the identity, yields and sequence of appearance of the reaction products in UHV, which can include H_2O, H_2, CO, CO_2 and O We propose reaction mechanisms for various metal surfaces and categorize the metals according to their reactivity for HCOOH decomposition Au and Ag are the least reactive, while Pd(100) and W(100) are most reactive, according to our criteria

Acknowledgments

Acknowledgment is made to the Donors of the Petroleum Research Fund, administered by the American Chemical Society This work was also supported by the Director for Energy Research, Office of Basic Energy Sciences Ames Laboratory is operated for the US Department of Energy by Iowa State University under Contract W-7405-Eng-82 We also thank R J Madix for useful comments

References

1 E Mueller, Z Elektrochem , 29 (1923) 264
2 E Mueller, Z Elektrochem , 33 (1927) 561
3 E Mueller and S Tanaka, Z Elektrochem , 34 (1928) 256
4 K Schwabe, Z Elektrochem , 61 (1957) 744
5 M W Breiter, Electrochemical Processes in Fuel Cells, Springer, Berlin, 1969
6 B B Damaskin, O A Petrii and V V Batrakov, Adsorption of Organic Compounds on Electrodes, Plenum, New York, 1971
7 W Vielstich, Fuel Cells, Wiley, London, 1970
8 A Capon and R Parsons, J Electroanal Chem , 44 (1973) 1
9 R Parsons and T VanderNoot, J Electroanal Chem , 257 (1988) 9
10 S -C Chang, Y Ho and M J Weaver, Surf Sci , 265 (1992) 81
11 P Mars, J J F Scholten and P Zwietering, Adv Catal , 14 (1963) 35
12 J M Trillo, G Munuera and J M Criado, Catal Rev , 7 (1972) 51
13 J McCarty, J Falconer and R J Madix, J Catal 30 (1973) 235
14 D P Woodruff and T A Delchar, Modern Techniques of Surface Science, Cambridge University Press, New York, 1986
15 G Ertl and J Kuppers, Low Energy Electrons and Surface Chemistry, VCH, Darmstadt, 1985
16 N Kizhakevariam and E M Stuve, Simulating electrochemical reactions in ultrahigh vacuum, in D Scherson, M Daroux, D Tryk and X Xing (Eds), Proc Workshop on Structural Effects in Electrocatalysis and Oxygen Electrochemistry, The Electrochemical Society, Pennington, NJ 1992, pp 40–61

17 E M Stuve and N Kizhakevariam, J Vac Sci Technol A, 11 (1993) 2217
18 E M Stuve, K Bange and J K Sass, Double layer simulation studies in ultrahigh vacuum coadsorption of water and electropositive and electronegative adsorbates on Ag(110) and Cu(110), in A F de Silva (ed), Trends in Interfacial Electrochemistry, Reidel, Dordrecht, 1986, pp 255–280
19 J K Sass, D Lackey and J Schott, Electrochim Acta, 36 (1991) 1883
20 F T Wagner and T E Moylan, Modeling the aqueous/metal interface in ultrahigh vacuum via cryogenic coadsorption, in M P Soriaga (ed), Electrochemical Surface Science Molecular Phenomena et Electrode Surfaces, ACS symp Series 378, American Chemical Society, Washington, DC, 1988, Ch 5
21 F T Wagner and T E Moylan, Electrochemical double layer simulations in ultrahigh vacuum, in D Scherson, D Tryk, M Daroux and X Xing (eds), Proc Workshop on Structural Effects in Electrocatalysis and Oxygen Electrochemistry, The Electrochemical Society, Pennington, NJ, 1992, pp 25–39
22 F T Wagner, Simulation of the electrical double layer in ultrahigh vacuum, in J P Lipkowski and J P N Ross (eds), The Structure of Electrified Interfaces, Frontiers of Electrochemistry 2, VCH, Darmstadt, 1993
23 R J Madix, Adv Catal , 29 (1980) 1
24 B A Sexton and R J Madix, Surf Sci , 105 (1981) 177
25 D A Outka and R J Madix, Surf Sci , 179 (1987) 361
26 M Bowker and R J Madix, Surf Sci , 102 (1981) 542
27 B E Hayden, K Prince, D P Woodruff and A M Bradshaw, Surf Sci , 133 (1983) 589
28 F C Henn, J A Rodriguez and C T Campbell, Surf Sci , 236 (1990) 282
29 W Erley and D Sander, J Vac Sci Technol A, 7 (1989) 2238
30 J L Falconer and R J Madix, J Catal , 51 (1978) 47
31 E I Ko and R J Madix, Appl Surf Sci , 3 (1979) 236
32 F Solymosi and I Kovacs, Surf Sci , 259 (1991) 95
33 J L Davis and M A Barteau, Surf Sci , 256 (1991) 50
34 N Kizhakevariam and E M Stuve, J Vac Sci Technol A, 8 (1990) 2557
35 N R Avery, Appl Surf Sci , 11–12 (1982) 774
36 N Abbas and R J Madix, Appl Surf Sci , 16 (1983) 424
37 M R Columbia and P A Thiel, Surf Sci , 235 (1990) 53
38 F Solymosi, J Kiss and I Kovacs, Surf Sci , 192 (1987) 47
39 Y -K Sun and W H Weinberg, J Chem Phys , 94 (1991) 4587
40 L A Larson and J T Dickinson, Surf Sci , 84 (1979) 17
41 M B Jensen, U Myler and P A Thiel, Surf Sci , 290 (1993) L655
42 R W Joyner and M W Roberts, Proc R Soc London, Ser A, 350 (1976) 107
43 F Holtzberg, B Post and I Fankuchen, Acta Crystall , 6 (1953) 127
44 R C Millikan and K S Pitzer, J Am Chem Soc , 80 (1958) 3515
45 Y Mikawa, R J Jakobsen and J W Brasch, J Chem Phys , 45 (1966) 4750
46 Y Mikawa, J W Brasch and R J Jakobsen, J Molec Spectrosc , 24 (1967) 314
47 B A Sexton, Surf Sci , 88 (1979) 319
48 M R Columbia, A M Crabtree and P A Thiel, J Am Chem Soc , 114 (1991) 1231
49 M Chtaib, P A Thiry, J J Pireaux, J P Delrue and R Caudano, Surf Sci , 162 (1985) 245
50 C Houtman and M A Barteau, Surf Sci , 248 (1991) 57
51 R J Madix, J Falconer and J McCarty, J Catal , 31 (1973) 316
52 J L Falconer, J G McCarty and R J Madix, Surf Sci , 42 (1974) 329
53 J L Falconer and R J Madix, Surf Sci , 46 (1974) 473
54 R J Madix and J L Falconer, Surf Sci , 51 (1975) 546
55 J McCarty and R J Madix, J Catal , 38 (1975) 402
56 J L Falconer and R J Madix, Surf Sci , 48 (1975) 393
57 S W Johnson and R J Madix, Surf Sci , 66 (1977) 189
58 J B Benziger and R J Madix, Surf Sci , 79 (1979) 394
59 N R Avery, B H Toby, A B Anton and W H Weinberg, Surf Sci , 122 (1982) L574
60 B H Toby, N R Avery, A B Anton and W H Weinberg, J Electron Spectrosc , 29 (1983) 317
61 R J Madix, J L Gland, G E Mitchell and B A Sexton, Surf Sci , 125 (1983) 481
62 T S Jones, N V Richardson and A W Joshi, Surf Sci , 207 (1988) L948
63 T S Jones, M R Ashton and N V Richardson, J Chem Phys , 90 (1989) 7564
64 J B Benziger and G B Schoofs, J Phys Chem , 88 (1984) 4439
65 D H S Ying and R J Madix, J Catal , 61 (1980) 48
66 L H Dubois, T H Ellis, B R Zegarski and S D Kevan, Surf Sci , 172 (1986) 385
67 B A Sexton, J Vac Sci Technol , 17 (1980) 141
68 B E Hayden, K Prince, D P Woodruff and A M Bradshaw, Phys Rev Lett , 51 (1983) 475
69 J Stoehr, D A Outka, R J Madix and U Doebler, Phys Rev Lett , 54 (1985) 1256
70 D A Outka, R J Madix and J Stohr, Surf Sci , 164 (1985) 235
71 M D Crapper, C E Riley and D P Woodruff, Phys Rev Lett , 57 (1986) 2598
72 M D Crapper, C E Riley and D P Woodruff, Surf Sci , 184 (1987) 121
73 D P Woodruff, C F McConville, A L D Kilcoyne, T Linder, J Somers, M Surman, G Paolucci and A M Bradshaw, Surf Sci , 201 (1988) 228
74 S P Mehandru and A B Anderson, Surf Sci , 219 (1989) 68
75 L S Caputi, G Chiarello, M G Lancellotti, G A Rizzi, M Sambi and G Granozzi, Surf Sci , 291 (1993) L756
76 A Puschmann, J Haaase, M D Crapper, C E Riley and D P Woodruff, Phys Rev Lett , 54 (1985) 2250
77 M D Crapper, C E Riley, D P Woodruff, A Puschmann and J Haase, Surf Sci , 171 (1986) 1
78 E G Seebauer, A C F Kong and L D Schmidt, Appl Surf Sci , 29 (1987) 380
79 P Hofmann, S R Bare, N V Richardson and D A King, Surf Sci , 133 (1983) L459
80 N R Avery, Appl Surf Sci , 14 (1982-83) 149
81 M R Columbia, A M Crabtree and P A Thiel, J Electroanal Chem , 351 (1993) 207
82 U Myler, M B Jensen and P A Thiel, in preparation
83 M R Columbia, A M Crabtree and P A Thiel, J Electroanal Chem , 345 (1993) 93
84 S W Jorgensen and R J Madix, J Am Chem Soc , 110 (1988) 397
85 D Sander and W Erley, J Vac Sci Technol A, 8 (1990) 3367
86 C Egawa, I Doi, S Naito and K Tamaru, Surf Sci , 176 (1986) 491
87 F Solymosi, J Kiss and I Kovacs, J Vac Sci Technol A, 5 (1987) 1108
88 F Solymosi, J Kiss and I Kovacs, J Phys Chem , 92 (1988) 796
89 M A Barteau, M Bowker and R J Madix, Surf Sci , 94 (1980) 303
90 P A Stevens, R J Madix and J Stoehr, Surf Sci , 230 (1990) 1

91 D A Outka and R J Madix, J Am Chem, Soc, 109 (1987) 1708
92 M Chtaib, J P Delrue and R Caudano, Phys Scr, T4 (1983) 133
93 M Chtaib, P A Thiry, J P Delrue, J J Pireaux and R Caudano, J Electron Spectrosc, 29 (1983) 293
94 N D S Canning, D Outka and R J Madix, Surf Sci, 141 (1984) 240
95 L E Davis, N C MacDonald, P W Palmberg, G E Riach and R E Weber, Handbook of Auger Electron Spectroscopy, (Perkin–Elmer, Eden Prairie, MN, 1978)
96 J B Benziger and R J Madix, J Catal, 65 (1980) 49
97 J B Benziger and R J Madix, J Catal, 74 (1982) 67
98 J B Benziger, E I Ko and R J Madix, J Catal, 58 (1979) 149
99 A K Bhattacharya, J Chem Soc, Faraday Trans 1, 75 (1979) 863
100 P A Thiel and T E Madey, Surf Sci Rep, 7 (1987) 211